

Predicting Potential Fires in Indonesia by Analyzing VIIRS Night Data during 2018 – 2022

Basuki Suhardiman^{a,b,*} and Benni Rio Hermanto^c

^a*Directorate of Information Technology, Institut Teknologi Bandung,
Jl Ganesha 10, Bandung, Indonesia*

^b*Master's Program in Computational Science, Faculty of Mathematics and Natural Sciences, Institut
Teknologi Bandung,
Jl Ganesha 10, Bandung, Indonesia*

^c*Biomedical Engineering Department, School of Electrical Engineering and Informatics, Institut
Teknologi Bandung*

E-mail: basuki@itb.ac.id, benirio@itb.ac.id

Forest fires have been detected to occur in Indonesia since 1998. The forest fires mostly resulted from human activities in order to expand their land, especially oil palm lands. Once a land clearing is carried out, it covers areas of tens to hundreds of thousands of hectares. The peak of the forest fires occurred in 2015 when almost half of the world was affected especially by smoke from the fire. In 2011, VIIRS (Visible Infrared Imaging Radiometer Suite) was launched by NOAA (National Oceanic and Atmospheric Administration). In their collected data, there is data on Indonesia issued daily for areas in the islands of Java, Sumatra, Kalimantan, Sulawesi, and the general areas of Indonesia. The VIIRS night data shows the possibility of some burning at night. We need to identify burnings that potentially become fires, which are potentially producing smoke. It is important to observe areas where large-scale forest fires frequently occur, so the authority could do some prevention beforehand. Using existing data released per day per area, we utilize an ANN (Artificial Neural Network) to identify a potential fire. The processes start with data cleaning and processing, Neural Network creation, and finally ANN training and testing. By using the ANN prediction model with the MinMax Scaler, we choose variables Temperature, Radiant Heat Intensity, and Source Footprint. Simulations are made to show the ranges of these variables that predict the possibility of 'flame' status occurring. We conclude that the ANN method can give more accurate results than the existing classification.

*International Symposium on Grids and Clouds (ISGC) 2023,
19 - 31 March 2023
Academia Sinica Taipei, Taiwan*

*Speaker

1. Introduction

Massive forest fires have been occurring and causing environmental impacts in almost all Asian countries in the past and present decade. The forest fires that occurred in Indonesia, especially those that occurred in 2015, have had a bad impact, not only on the Indonesian territory, but also on neighboring countries such as Singapore, Malaysia, and Thailand. This impact was also felt by almost half of the world. As reported by the Global Fire Watch [1], forest fires in Indonesia in 2015-2016 occurred mainly in peatlands, especially in Sumatra and Kalimantan. For the Riau province, fires have almost hit 47% of the Riau province. Using remote sensing techniques, authors in [2] investigated the worst air quality levels at a regional scale caused by a forest fire event in Balochistan, Pakistan's Largha Sherani District. Having observed the impact of forest fires on the ecology, environment, and socioeconomics of nations across the globe, authors [3] urged the G20 nations should step forward to build and improve bilateral and or multilateral cooperation and coordination, as well as exchange enough financial resources, technology, and training among themselves, in order to lessen the effects of forest fires on the environment and socioeconomics.

Research has been conducted to predict the potential factors of forest fires. Authors in [4] evaluated and mapped the forest fire susceptibility zones in Uttarakhand, a hilly state in Western Himalayas, by utilizing geospatial methodologies, machine learning algorithms (MLA), and deep learning-based sensitivity and uncertainty analyses. Results showed that the significant factors included evapotranspiration, yearly rainfall, wind speed, distance to agriculture, distance to tourist attractions, distance to built-up areas, etc. They suggest strict control and monitoring of these parameters can stop the susceptibility to forest fires. Based on the examination [1] in Indonesia, some people are often intentionally set on fire to facilitate the cultivation of a new site for agricultural expansion or force people away during land disputes.

Based on [5], three main elements influencing forest fire behavior are combustibles, geography, and weather, and contemporary forest fire spread models must take weather aspects into full consideration. The study in [5] suggested a forest fire spread approach based on ambient meteorological elements, in order to give a graphical simulation of forest fire spread in the natural environment. The study also offered a forest fire spread technique based on environmental weather elements, in order to enhance the connected senses' sense of immersion and to enable realistic scene wandering.

In 2011, NOAA (National Oceanic and Atmospheric Administration) began to operate one of the remote sensing technologies called VIIRS (Visible Infrared Imaging Radiometer Suite) [6], which was produced by the Raytheon Company. It is a sensor mounted on the polar-orbiting Suomi National Polar-orbiting Partnership (Suomi NPP), NOAA-20, and NOAA-21 meteorological satellites, and is now being used by more researchers, including [7–10]. In 2018, a new product of VIIRS was released, namely the VIIRS Nighttime Imagery, which collects the earth's surface and atmosphere by utilizing a sensor created to catch low-light emission Sources under a variety of lighting situations. With worldwide coverage every 14 hours, VIIRS is able to provide two data processing streams that result in two distinct sets of land products. One is created by NOAA and gives the National Weather Service operational data to utilize, which are known as EDR (Environmental Data Records). The second stream, which comes from NASA, aims to benefit the greater scientific community. VIIRS data from NOAA is made available by NASA and NOAA and is already available in KML or CSV format. Locational information (latitude, longitude),

confidence, temperature (Kelvin), and FRP (Fire Radiative Power) in MW are all included in this data.

In this paper, we propose to identify potential fires in areas of Indonesia using data of the Visible Infrared Imaging Radiometer Suite (VIIRS) retrieved from EOS (Earth Observation Group, School of Colorado (Mines.edu) [11]. By using the ANN prediction model based on the concept of MinMax Scaler, the variables being observed are temperature, radiant heat intensity, and Source Footprint. The neural network being used is two hid-den layers with each hidden layer using 10 neurons. Having had a good accuracy on training data, we use it to simulate the identification of “flame” or “no flame” on ranges of those determined variables and analyze the results.

2. Visible Infrared Imaging Radiometer Suite (VIIRS)

VIIRS is unique in the recording of near-infrared and short-wave infrared data at night. This includes the M7, M8, and M10 spectral bands. Nighttime M11 data became available in December 2017. With sunlight eliminated, combustion Sources are easily detected, especially in the M10 and M11 bands. The recorded signal can be fully attributed to the combustion Source. We use data from all of the VIIRS bands collecting data at night. The data from M10, M11, M12, and M13 bands are used to detect combustion Sources. To eliminate noise, confirmation is sought in the Day/Night Band (DNB), M7 and M8. Plank curve fitting is performed to estimate the temperature of the background and hot Sources. The special combustion data is taken at night local time in this case specifically for Indonesia. There are four (4) major islands whose data is observed per day, which are the Islands of Sumatra, Kalimantan, Sulawesi, and Java. Special observation is especially in the islands of Sumatra and Kalimantan because these two areas are usually the site of extensive forest fires, as well as oil palm plantations. Cases of forest fires in Indonesia are dominated by these two regions. Based on data obtained for years, there have been quite massive forest fires in these areas.

Based on [10–12], the temperature being calculated by the VNF (VIIRS Night-fire) ranges from nearly 700 K and extends past 2000 K. VNF’s Source area detection limits are highly dependent on temperature and range from 53 m² at 700 K to the 0.26 m² at 1800 K, the typical temperature of natural gas flaring. Source area detection limits decline as temperature increases, an expression of the T⁴ term present in the Stefan–Boltzmann Law. The low-temperature VNF cluster runs from 700 to 1500 K and is dominated by biomass burning. There is a high-temperature VNF cluster ranging from 1500 to 2100 K dominated by gas flaring. In contrast, the DNB has limited capabilities to detect low-temperature biomass burning in the range below 750 K, but exceedingly low detection limits beyond 1000 K, reaching Source areas of 0.01 m² at 1500 K. At the typical temperature found for natural gas flaring (1800 K) the DNB detection limit is 0.001 m², substantially smaller than the M10 detection limit of 0.26 m².

Figure 1 shows the placemark icons in the downloaded KMZ file that classifies the temperature range of the detected fire. Data structures in the KML file consist of several factors, which are latitude, longitude, time, temperature, temperature background, radiant heat intensity, radiant heat, Source Footprint, local time, cloud state, and atmosphere corrected.

An example of collected data is shown in Table 1. Latitude and longitude show detailed locations. Time indicates the time the data was retrieved in GMT+7 format. Temperature shows the

| KMZ Placemark | Definition |
|---|--------------------------|
|  | Non-confirming detection |
|  | 400K < T < 1000K |
|  | 1000K < T < 1200K |
|  | 1200K < T < 1400K |
|  | 1400K < T < 1600K |
|  | 1600K < T < 2500K |
|  | 2500K < T |

Figure 1: Flag Icons based on the temperature range

Table 1: An example of data

| Latitude & Longitude | Time (local time, GMT+7) | Temperature (K) | Radiant Heat Intensity (W/m ²) | Source Footprint (m ²) | Flag Icon | Label |
|-------------------------|--------------------------|-----------------|--|------------------------------------|-----------|----------|
| -0.085922 125.161415 | 20190404 16:08:36 | 899 | 1.41 | 102.13 | Purple | No Flame |
| -1.318696 131.020905 | 20190404 16:08:42 | 1545 | 2.13 | 9.01 | Yellow | No Flame |
| 1.526250 109.116936 | 20190404 17:49:15 | 769 | 5.53 | 203.07 | Purple | No Flame |
| -1.459049 127.433899 | 20190924 17:06:08 | 1648 | 113.52 | 196.97 | Red | Flame |
| -2.439352 133.139923 | 20190419 16:27:46 | 1778 | 77.56 | 80.30 | Red | Flame |

measured temperature in Kelvin; background temperature shows the measured temperature around the location. Radiant Heat Intensity in W/m² units shows heat intensity measured in Watts per square meter. Source Footprint shows the area of heat that occurs at the time of measurement in m². There are other measures in the source data, which are Cloud State, which indicates the presence or absence of clouds at the location, and Atmosphere Corrected, which is a flag being issued to indicate a correction to the atmospheric conditions. In this research, we only use Temperature, Radiant Heat Intensity, and Source Footprint.

2.1 Data preprocessing

Having been released daily by mines.edu, the data from NOAA using VIIRS is quite complete and describes the conditions at the observed locations, which consist of four zones in Indonesia; Sumatra, Kalimantan, Sulawesi, and Java. The data format is in KMZ file, so it must be converted to KML and then to CSV file using the MySQL program. We collected 17,532 data from dates

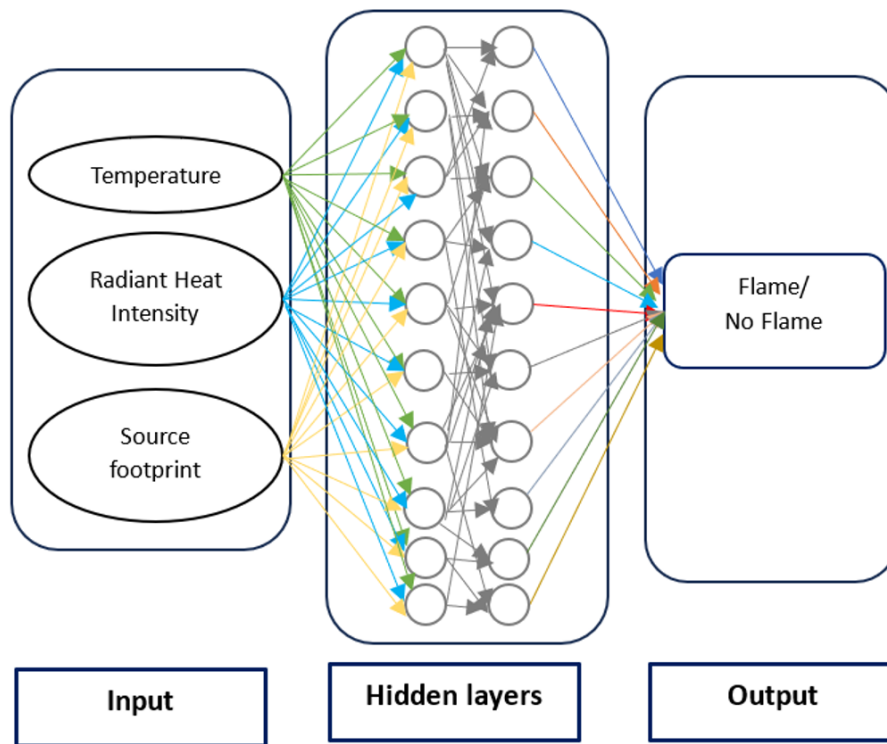


Figure 2: Model Development Scheme

April 4, 2019 – September 25, 2019, which are the results of afternoon surveillance from 15:25:27 to 20:01:10 GMT+7. An example of this data is shown in Table 1.

In Table 1, the icons are the estimated range of the fire temperature on a certain scale in Kelvin units. These icons are represented by colored pictures to indicate the temperature range at the point of fire. The output label is made using flame or no flame criteria with reference to the temperature range detected in the data using icons. Flame is only indicated by temperatures higher than 1600 K. This label will be tested using our ANN method.

2.2 Artificial Neural Network Model

Using the training data from previous assessments using VIIRS, the ANN model being used consists of inputs: Temperature (K), Radiant Heat Intensity (W/m^2), and Source Footprint (m^2). The expected output is 'flame' or 'no flame'. In Figure 2, the input consisting of 3 variables is entered into two hidden layers and the resulting output is a flame prediction.

It shown in Table 1, the existing flame label is limited to the condition of the red icon, which is in the range of 1600 K to 2500 K. By building a model with the input datasets, the model built using a neural network is expected to be able to predict more accurately the occurrence of a potential fire, which is by detecting its output flame (flame or no flame). We use the Python program with the scikit learn (sklearn) library tools which is a supervised learning neural network approach.

Table 2: Results of prediction

| No | Temperature (K) | Radiant Heat Intensity (W/m ²) | Source Footprint (m ²) | Result |
|----|-----------------|--|------------------------------------|----------|
| 1 | 1000 | 2000 | 10 | flame |
| 2 | 750 | 485.5 | 0 | flame |
| 3 | 1250 | 1000 | 200 | flame |
| 4 | 600 | 2000 | 200 | flame |
| 5 | 600 | 2000 | 500 | flame |
| 6 | 650 | 350 | 80 | no flame |
| 7 | 700 | 9 | 2 | no flame |
| 8 | 600 | 6.88 | 667.09 | no flame |
| 9 | 600 | 6.88 | 10 | no flame |

3. Data Training and Testing

We define the half of data as training data and the rest as test data. On the training data, we use the MLPClassifier, which is a neural network algorithm that can learn to classify data. In this case, it is being trained on the dataTrain and labelTrain data using the solver 'lbfgs', alpha=1e-5, and two hidden layers with 10 neurons in each layer. The random_state parameter sets the seed for the random number generator used by the algorithm so that the results can be replicated. A Multi-Layer Perceptron (MLP) classifier on some datasets is using the scikit-learn library in Python. The dataset seems to contain three features: 'Temp', 'Radian', and 'Source', and also a binary label ('label').

The MinMaxScaler function is used to scale the features to a range between 0 and 1, to make sure that all features are on the same scale and have the same weight in the model. Let l_u and l_d are respectively the maximum and minimum values of a variable. If x is a real value variable, the scaled value y is calculated as follows.

$$y = \frac{x - l_d}{l_u - l_d}, \quad (1)$$

so $0 \leq y \leq 1$. The MLPClassifier function is used to create a neural network with two hidden layers, each containing 10 neurons. The 'lbfgs' solver is used to optimize the weights, and 'alpha' is used to set a regularization parameter. Finally, the model is "fit" to the training data using the fit command. The remaining code calculates the accuracy of the model on the test data. The predictions are made for each instance in the test data using the "predict" command, and the number of "correct" predictions is stored in the correct variable. The accuracy is then calculated as the ratio of correct predictions to the total number of test instances, and printed out as a percentage.

The MLPClassifier neural network process in the Sklearn program is based on the Python language, using Min_Max_Scaler to test data and using clf.predict to predict data accuracy. The obtained results produce an accuracy of 99.98% for the labels 'flame' and 'no flame'. The resulting training and tests will be used to perform fire analysis and predictions.

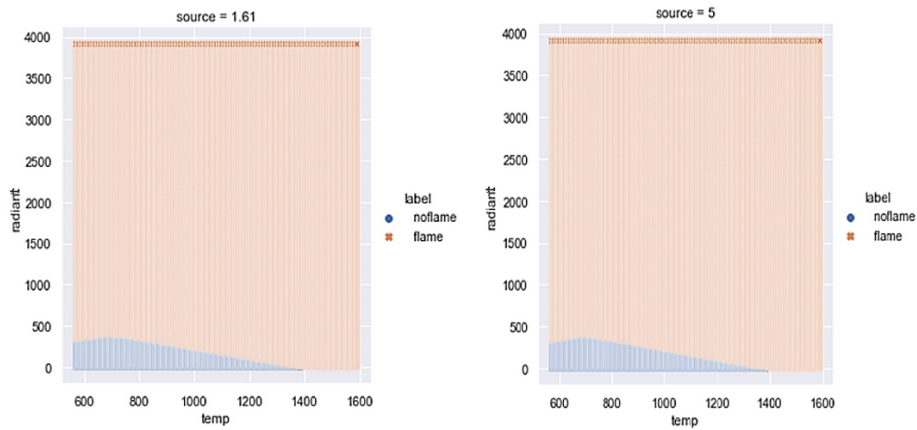


Figure 3: Source Footprint of 1.61 m² (left) and 5 m² (right).

3.1 Simulation of Prediction

The range of each variable is the following: Temperature 563 K - 1964 K, Radiant Heat Intensity 0.32 W/ m² - 3927.4 W/ m², and Source Footprint 1.61 m² - 62680 m². Table 2 shows predictions for some values of the inputs. It shows some output is flame even though the temperature is below 1600 K, so it is an improved classification from Table 1. There are several conditions that produce a 'no flame' prediction. For example, predictions 8 and 9, which are at a temperature of 600 K with a radiant heat intensity of 6.88 W/m² and a Source Footprint of 10 m², are both producing 'no flame' predictions. So it is interesting to find the particular ranges of temperature and radiant heat intensity that give different outputs.

Now we determine discrete ranges of inputs for more simplified numerical simulations using Python and plot the obtained area. For the simulation, the range of Temperature is given from 570 K to 1590 K which increases every 10 K. Radiant Heat Intensity is given from 1 W/m² to 3911 W/m² which increases every 10 W/m². We only set particular values of Source Footprint in order to see some property of the result. For a certain value of Source Footprint, it resulted in fairly long rows of 40,376 lines. In the next section, we discuss the results plotted in the 'flame' and 'no flame' classifications.

4. Discussion

Figures 3-5 illustrate the classification resulting from our trained neural network for different values of the Source Footprint. The respective classification results as a function of Temperature (temp, horizontal axis) and Radiant Heat Intensity (radiant, vertical axis) are visualised by colour coding (pastel red: 'flame', pastel blue: 'no flame'). Most of the plot area is dominated by 'flame' status. It is quite a surprising result because the range of temperature is below 1600 K. On the other hand, 'no flame' status can be found for Temperatures larger than 1600 K. We also find that the larger the value of the Source Footprint, the wider the area of 'no flame'. It is clearly shown in Table 3, where the status of 'no flame' output is counted. There are only 1958 statuses of 'no flame' for the Source Footprint of 1.61 m². For the Source Footprint of 2000 m², there are 4665 statuses of 'no flame'.

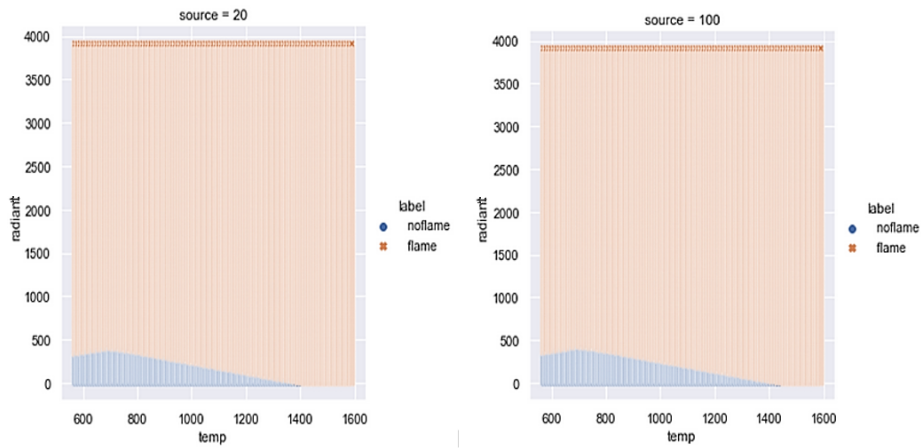


Figure 4: Source Footprint of 20 m² (left) and 100 m² (right).

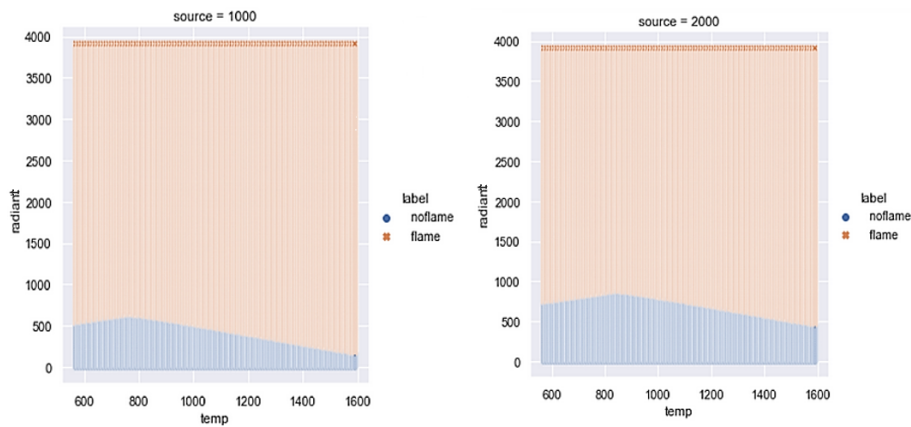


Figure 5: Source Footprint of 1000 m² (left) and 2000 m² (right).

Table 3: Count of no flame with various values of Source Footprint

| Source Footprint (m ²) | Flame status | Count |
|------------------------------------|--------------|-------|
| 1.61 | no flame | 1958 |
| 5 | no flame | 1965 |
| 10 | no flame | 1978 |
| 100 | no flame | 1999 |
| 1000 | no flame | 2188 |
| 2000 | no flame | 4665 |

Observing the threshold from 'flame' to 'no flame' in terms of Radiant Heat Intensity in all figures, we find - interestingly - that it is a curve increasing for a while as a function of Temperature and then decreasing. For example in the right Figure 5 for the Source Footprint of 5 and the Radiant Heat Intensity of 350, the range 560 – 600 gives 'flame' status, the range 610 – 830 gives 'no flame' status, and then the range 840 – 1600 gives 'flame' status again. It shows that the intervals of temperature implying a 'flame' vs. 'no flame' status at borderline Radiant Heat Intensities deserve special attention.

5. Conclusion

This study proposes data processing for data indicating potential wildfires (in particular VIIRS data) using an Artificial Neural Network (ANN) with two hidden layers with each hidden layer using 10 neurons. The use of the 'lbgs' optimizer solver has resulted in an accuracy rate for the 'flame' and 'no flame' labels reaching 99.98%. The existing definition of the 'flame' status is a condition with a temperature between 1600 Kelvin to 2500 Kelvin. Using the simulation in the previous section, our result shows that the 'flame' status can be generated from temperatures ranging from 563 Kelvin to 1964 Kelvin, and 'no flame' status can be generated from temperatures higher than 1600 Kelvin. Considering the classification results as a function of Temperature and Radiant Heat Intensity (as first and second input variables to our ANN), the ANN tends more to 'no flame' classifications when the Source Footprint (as our third input variable) is larger. More precisely, the area on the Temperature / Radiant Heat Intensity plane in which the ANN suggests a 'no flame' status (at lower Radiant Heat Intensities) tends to increase with Source Footprint. In addition for certain values of Radiant Heat Intensity in the simulation, the 'flame' status can change to 'no flame' status, and back to 'flame' status, when the temperature is increasing. A more in-depth study is needed regarding these findings. We conclude that the ANN method can give more accurate results in a classification distinguishing 'no flame' and 'flame' burning conditions from parameters obtained from satellite observations.

References

- [1] A. Chamorro, S. Minnemeyer and S. Sargent. Exploring Indonesia's Long and Complicated History of Forest Fires, <https://globalforestwatch.org/blog/fires/indonesias-fire-history-provides-insight-to-prevent-future-fire/>
- [2] S. Tariq, H. Nawaz, U. Mehmood, Z. Haq, U.K. Pata, M. Murshed. Remote sensing of air pollution due to forest fires and dust storm over Balochistan (Pakistan), *Atmospheric Pollution Research*, Vol 14, Issue 2, 2023, 101674, ISSN 1309-1042, <https://doi.org/10.1016/j.apr.2023.101674>.
- [3] C.P. Kala. Environmental and socioeconomic impacts of forest fires: A call for multilateral cooperation and management interventions, *Natural Hazards Research*, 2023, ISSN 2666-5921. <https://doi.org/10.1016/j.nhres.2023.04.003>.

- [4] M. Rihan, A.A. Bindajam, S. Talukdar, Shahfahad, M.W. Naikoo, J. Mallick, and A. Rahman. Forest fire susceptibility mapping with sensitivity and uncertainty analysis using machine learning and deep learning algorithms, *Advances in Space Research*, 2023, ISSN 0273-1177.
- [5] Q. Meng, Y. Huai, J. You, X. Nie. Visualization of 3D forest fire spread based on the coupling of multiple weather factors, *Computers & Graphics*, Vol 110, 2023, Pages 58-68, ISSN 0097-8493, <https://doi.org/10.1016/j.cag.2022.12.002>.
- [6] Visible Infrared Imaging Radiometer Suite, https://en.wikipedia.org/wiki/Visible_Infrared_Imaging_Radiometer_Suite accessed in April 2023.
- [7] Y. Ma, B. Liu, W. Gong, Y. Shi, S. Jin. Impact of environmental pollution on the retrieval of AOD products from Visible Infrared Imaging Radiometer Suite (VIIRS) over Wuhan, *Atmospheric Pollution Research*, Vol 10, Issue 6, 2019, Pages 2063-2071, ISSN 1309-1042, <https://doi.org/10.1016/j.apr.2019.09.014>.
- [8] Y. Wan, Y. Chen, K. Li. Identification and spatiotemporal distribution analysis of global biomass burning based on Suomi-NPP VIIRS Nightfire data, *Journal of Cleaner Production*, Vol 359, 2022, 131959, ISSN 0959-6526, <https://doi.org/10.1016/j.jclepro.2022.131959>.
- [9] J. Wang, S. Roudini, E.J. Hyer, X. Xu, M. Zhou, L.C. Garcia, J.S. Reid, D.A. Peterson, A.M. da Silva, Detecting nighttime fire combustion phase by hybrid application of visible and infrared radiation from Suomi NPP VIIRS, *Remote Sensing of Environment*, Vol 237, 2020, 111466, ISSN 0034-4257, <https://doi.org/10.1016/j.rse.2019.111466>.
- [10] C.D. Elvidge, F.C. Hue, M. Zhizhin, and K.E. Baugh. VIIRS Nightfire: Satellite pyrometry at night. *Remote Sensing* 5, no. 9 (2013): 4423-4449. <https://eogdata.mines.edu/products/vnf/>.
- [11] . C.D. Elvidge, M. Zhizhin, K. Baugh, F.C. Hsu, and T. Ghosh. Extending Night-time Combustion Source Detection Limits with Short Wavelength VIIRS Data. *Remote Sens.* 2019, 11, 395. <https://doi.org/10.3390/rs11040395> Fire Radiated Power (FRP), <https://bg.copernicus.org/articles/16/275/2019/>
- [12] Use of Night time VIIRS data for Fire Mapping, Christopher D. Elvidge, <https://payneinstitute.mines.edu/wp-content/uploads/sites/149/2019/11/Chris-Elvidge-Presentation.pdf>
- [13] VIIRS Night, Earth Observation Group, <https://eogdata.mines.edu/products/vnf/>
- [14] Pedregosa, F., Varoquaux, G., Gramfort, A., Michel, V., Thirion, B., Grisel, O., Blondel, M., Prettenhofer, P., Weiss, R., Dubourg, V., Vanderplas, J., Passos, A., Cournapeau, D., Brucher, M., Perrot, M., and Duchesnay, E. Scikit-learn: Machine Learning in Python. *Journal of Machine Learning Research*, Vol 12, pages 2825-2830, 2011, https://scikit-learn.org/stable/modules/neural_networks_supervised.html
- [15] C. D. Elvidge, K. E. Baugh, M. Zhizhin, and F.-C. Hsu, "Why VIIRS data are superior to DMSP for mapping nighttime lights," *Asia-Pacific Advanced Network* 35, vol. 35, p. 62, 2013.

- [16] Elvidge, Christopher D., Kimberly Baugh, Mikhail Zhizhin, Feng Chi Hsu, and Tilottama Ghosh. "VIIRS night-time lights." *International Journal of Remote Sensing* 38, no. 21 (2017): 5860-5879.
- [17] C. D. Elvidge, M. Zhizhin, T. Ghosh, F-C. Hsu, "Annual time series of global VIIRS nighttime lights derived from monthly averages: 2012 to 2019", *Remote Sensing* (In press)

POS (ISGC&HEP I X 2 0 2 3) 0 2 5